Femtosecond laser pulse irradiation of solid targets as a general route to nanoparticle formation in a vacuum

S. Amoruso, G. Ausanio, R. Bruzzese, M. Vitiello, and X. Wang
Coherentia - INFM and Dipartimento di Scienze Fisiche, Univerità di Napoli Federico II, Complesso Universitario di Monte S. Angelo, Via Cintia, I-80126 Napoli (Italy)
(Received 29 June 2004; published 21 January 2005)

By studying the fs laser produced plume of different materials we show experimentally that the process of matter removal during ultrashort (fs) laser pulse irradiation followed by vacuum expansion is characterized by a number of general features, whichever the nature of the target material. In particular, fs laser ablation of solid targets at laser intensities of the order of $10^{12}-10^{13}$ W/cm^2, inevitably leads to the generation of nanoparticles of that material. This has been evidenced by atomic force microscopy analysis of less than one layer deposits showing that the produced nanoparticles have mean radii generally in the range 5–25 nm, with pretty narrow size distributions. These results are in very good agreement with the physical description and numerical predictions of recently published theoretical analyses of fs ablation processes.

DOI: 10.1103/PhysRevB.71.033406 PACS number(s): 79.20.Ds, 52.38.Mf

The field of nanoscience has recently attracted a great deal of attention from the scientific community due to the great variety of electrical and mechanical properties presented by *nanostructures* which give rise to interesting physical phenomena and can be exploited for the development of different technological applications.[1–4] In particular, nanoparticles (NP's) of different elements and compounds have unique properties, and their synthesis and study is of great interest for both technological applications and fundamental research. Among the traditional techniques for producing NP's and NP's films one can quote arc discharge, and vapor and electrochemical deposition. In the last years, pulsed laser deposition (PLD) has also gained some interest in this respect because of a number of advantages over other processes, such as the possibility of producing materials with a complex stoichiometry, and a narrower distribution of NP's size as well as a reduced porosity. Typically, PLD is carried out in an ambient gas used to quench the ablated plume, thus controlling the mean particle size (see Ref. 5, e.g.). This technique, however, presents the disadvantage of requiring a specific optimization of the background gas pressure, and of introducing the need to address complex aspects of the expansion of the plume into the ambient gas such as its gasdynamics, and "in-flight" chemical kinetics.

In the last couple of years a different PLD technique based on fs laser irradiation of solid targets in vacuum has been used as a means for the synthesis of NP's in the specific cases of Si and Ge,[6,7] and of Al and Ti.[8,9] In addition to these experimental results, several recent theoretical studies have suggested that the rapid expansion and cooling of solid-density matter irradiated by a fs laser pulse may result in NP's generation via different mechanisms. In particular, liquid phase ejection and fragmentation, homogeneous nucleation and decomposition, and spinodal decomposition may all lead to NP's production in solid targets under different heating regimes.[10–14] The use of fs laser ablation for NP's synthesis in vacuum can be attractive for several reasons. First, and contrary to what happens with longer pulses (ns, and ps time scales), fs pulses do not interact with the ejected material thus avoiding complicated secondary laser interactions. Second, fs laser pulses heat a solid to higher temperature and pressure than do longer pulses of comparable fluence, since the energy is delivered before significant thermal conduction. Therefore a fs laser pulse can heat any material to a solid-density plasma state with temperature and pressure above the critical point, and is thus ideal for studying the fundamental properties of matter under extreme conditions. Finally, since the plume expansion takes place into vacuum, all the complications introduced by the presence of a background gas are avoided.

In the present study we show experimentally that different materials behave roughly the same when irradiated by femtosecond pulses at intensities around the threshold for plasma formation. In this condition, the very general mechanisms responsible for the ejection of matter always lead to the formation of NP's of the target material, with radii of tens of nm. This has been evidenced by atomic force microscopy (AFM) analysis of less than one layer deposits at room temperature of the material generated during fs laser ablation in vacuum of different materials of great basic and technological interest, such as noble metals (Au, Ag), ferromagnetic metals (Ni), semiconductors (Si), and even magnetic and superconducting multicomponents (TbDyFe and MgB_2).

In discussing our experimental findings we have particularly emphasized the general features which are always present and characterize the fs ablation process, whichever the target material, eventually leading to nanoparticles formation which turns out to be a specific aspect of matter removal during fs laser ablation of solid targets followed by expansion in vacuum. As a consequence, we can conclude that this technique lends itself as a different, general, and practical route to the production of NP's of different materials.

The experimental setup of the present analysis is similar to that reported in Ref. 7. The emission of a Ti:sapphire laser, producing $\approx$1-mJ–120-fs pulses at 780 nm, was focused to a spot size $\approx 2\times10^{-4}$ cm^2 on the sample surface, at an incidence angle of 45° and in *p* polarization. The target was

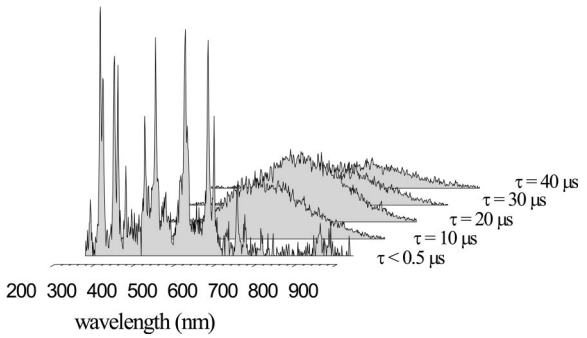

FIG. 1. Emission spectra of the fs gold plume for different time delays τ, at $d=1$ mm for a laser fluence $F=0.6$ J cm^{-2}.

mounted on a rotating holder and placed in a vacuum chamber evacuated to a residual pressure of $\approx 10^{-7}$ mbar. To characterize the ablation process, we have analyzed the light emitted by the plume leaving the target surface through a side window at right angles to the plume expansion direction. A slice of the plasma was imaged onto the entrance slit of a 1/4-m monochromator coupled to an intensified charge-coupled device (CCD) camera, with a minimum temporal gate of 5 ns and an overall spectral resolution of about 0.4 nm.

The plume was then deposited in high vacuum onto mica substrates at room temperature, parallel to the target, and located about 30 mm away. The deposited samples were analyzed with an AFM equipped with a sharpened silicon tip with a radius of less than 10 nm. The number of laser pulses used for deposition was carefully selected to obtain deposits of less than one layer in order to limit the influence of particles coalescence on the substrate. Thus the observed NP's size distributions can be safely assumed to reflect the actual size distribution of the free NP's expanding in vacuum and reaching the substrate.

The first general feature of the process of fs laser irradiation of a solid target at the intensities of concern here ($10^{12}-10^{13}$ W/cm^2) is shown in Fig. 1 in the representative case of Au. The emission spectra of the produced Au plume are reported as a function of the time delay τ with respect to the arrival of the laser pulse, at a representative distance $d=1$ mm, and for a laser fluence $F=0.6$ J/cm^2. The spectrum at short time delay ($\tau < 0.5$ μs) clearly indicates that emission from Au atoms dominates the plume luminescence on this short time scale. At longer time delays (5–100 μs), however, a structureless broad continuum emission is observed. Similar features of the emission spectra have been also observed at larger distances from the target surface (up to a few tens of mm).

This continuum, which is unfailingly observed with similar characteristics whichever the investigated target material (within the above quoted list), is due to emission from hot NP's produced during fs laser ablation, and provides a simple and useful technique to follow their dynamics in fs PLD. Hot NP's behave as a black-body radiator, and their emission is mainly determined by the temperature T of the system.[7] In particular, taking into account the NP's emissivity and that the CCD detector counts photons, for the spectral region of concern in the present study ($hc/\lambda \gg k_B T$) the emission intensity I is given by

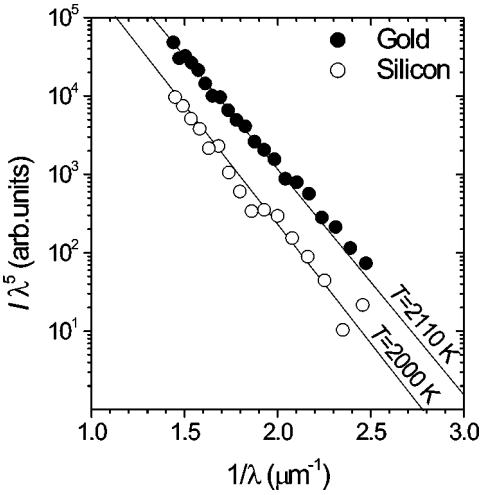

FIG. 2. Emission spectra of gold (•) and silicon (○) nanoparticles in $I\,\lambda^5-\lambda^{-1}$ coordinates on a semilogarithmic plot at a distance $d=1$ mm and a time delay $\tau=10$ μs. The straight lines are fitting curves according to Eq. (1), whose slopes give the temperature T.

$$I(\lambda) \propto \lambda^{-5} \exp\left(-\frac{hc}{\lambda \kappa_B T}\right), \tag{1}$$

where λ is the emission wavelength and h, k_B, and c are the Plank and Boltzmann constants, and the speed of light, respectively. As an example, Fig. 2 shows two typical and representative power spectra, in the case of Au and Si targets, in the form of log-linear plots of $(I\lambda^5)$ vs λ^{-1} registered at a distance $d=1$ mm at a time delay $\tau=10$ μs, for a laser fluence of ≈ 0.6 J/cm^2. One can see that the experimental points are well approximated by straight lines, whose slopes, according to Eq. (1), equal $hc/k_B T$, thus also providing an estimate of the nanoparticles temperature T. The values of the temperature are of the order of ≈ 2000 K for both targets, which is very plausible given the critical temperatures of gold and silicon.

We have also investigated the evolution of the nanoparticles temperature inside the expanding plume by measuring their emission spectra at different time delays and distances from the target surface. A very simple, phenomenological model of nanoparticles cooling during their vacuum expansion (see, e.g., Ref. 15 for the case of Si) leads to the conclusion that radiative cooling is always the most effective cooling mechanism in the late stages of plume expansion, independently of the nature of the target material.

The nanoparticles produced during fs laser ablation of different targets have then been deposited onto mica substrates to analyze their size and size distribution. As an example, Fig. 3(a) shows an AFM image of less than one layer of silver NP's deposited at a laser fluence of 0.6 J/cm^2, while Fig. 3(b) reports their size distribution, showing that they have a radius of less than 40 nm with a peak at ≈ 8 nm. Similar analyses have also been performed for the different targets considered in the present work (Ag, Au, Ni, Si, and TbDyFe) and at different laser fluences. Again, the general feature is that NP's of the target material are invariably pro-

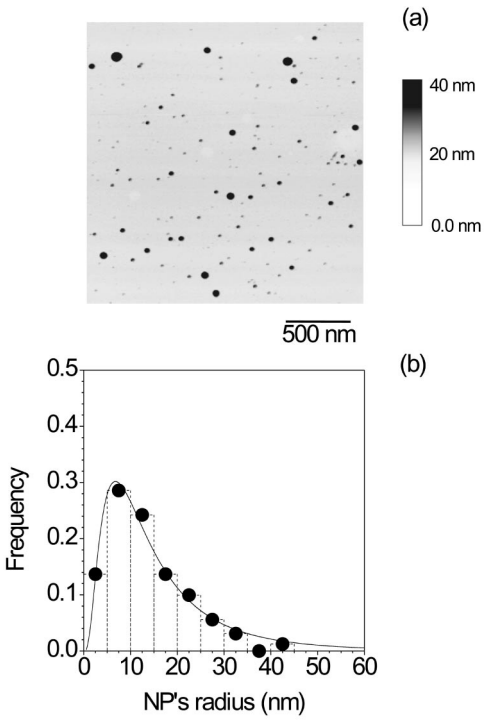

FIG. 3. (a) AFM image of Ag nanoparticles deposited in a high vacuum of $\approx 1\times10^{-7}$ mbar onto mica substrates. (b) Size histogram of Ag nanoparticles deposited under the experimental conditions shown in Fig. 3(a). The *solid* curve is a guide to the eye.

duced and deposited, with very similar sizes and size distributions.

The size statistics of the NP's for the different targets are summarized in Table I in terms of NP's mean radius R_m, standard deviation σ, and maximum radius $R_{\max}$. The maximum radius $R_{\max}$ represents the NP's size below which 90% of the particles are counted. Some features of the observed size distributions are particularly striking for their regularity, and interesting. For all materials, the mean NP's radius is of the order of 10–20 nm, with the only exception of TbDyFe at 0.6 J/cm^2. This specific aspect is in very good quantitative agreement with numerical predictions very recently appearing in the literature in the case of Si.[10] The size distributions are generally pretty narrow, with standard deviations/radius ranging from 0.5 to 0.8. Finally, in the investigated range, the general trend is for slightly increasing NP's mean radius R_m with increasing laser intensity. An almost similar behavior is observed for the maximum radius $R_{\max}$.

The very general features of ultrashort laser irradiation of solid targets evidenced by our results are consistent with the physical picture of the process outlined by the numerical predictions of very recent theoretical analysis devoted to the study of specific materials (mainly silicon and aluminum).

Under ultrashort laser pulse irradiation, the energy is delivered to matter in so short a time scale that absorption occurs at nearly solid-state density (near isochoric heating). The laser energy is first deposited in the electronic subsystem within a superficial layer with a thickness of tens of nm. Then, the energy is rapidly transferred from the electrons to the lattice on a time scale of few ps, and the heated region

TABLE I. Statistical parameters of the size distributions for three different values of the laser pulse fluence F. R_m is the nanoparticles mean radius and σ is the corresponding standard deviation. $R_{\max}$ is the maximum radius evaluated by considering the radius corresponding to 90% of the cumulative size distribution. α is the size distribution dispersion (i.e., $\alpha=\sigma/R_m$).

	F (J/cm^2)	I (W/cm^2)	R_m (nm)	σ (nm)	$R_{\max}$ (nm)	α
Au	0.3	2.5×10^{12}	8.0	4.7	27	0.59
Au	0.6	5.0×10^{12}	16.4	10.0	48	0.61
Au	1.2	1.0×10^{13}	14.1	10.9	55	0.77
Ag	0.3	2.5×10^{12}	11.8	8.5	46	0.72
Ag	0.6	5.0×10^{12}	13.4	8.0	45	0.60
Ag	1.2	1.0×10^{13}	15.1	11.6	52	0.77
Ni	0.3	2.5×10^{12}	19.7	13.8	60	0.70
Ni	0.6	5.0×10^{12}	17.4	11.0	55	0.63
Ni	1.2	1.0×10^{13}	24.7	19.4	100	0.78
Si	0.3	2.5×10^{12}	7.9	5.1	13	0.65
Si	0.6	5.0×10^{12}	11.6	8.6	15	0.75
Si	1.2	1.0×10^{13}	9.5	5.5	15	0.59
TbDyFe	0.6	5.0×10^{12}	44.8	24.8	80	0.55
TbDyFe	1.0	8.3×10^{12}	18.0	12.8	38	0.7

can reach high temperatures which are accompanied by a buildup of strong pressures within the material.[8,14] Next, a nearly adiabatic vacuum expansion of the heated material occurs with a consequent decrease of density and temperature. At this stage, the evolution of the system during this relaxation from the extreme excited state mainly depends on the material initial temperature, namely on the level of laser irradiation intensity. For example, the model developed in Ref. 8 for Al predicts that at laser intensities in the range 10^{12}–10^{13} W/cm^2, corresponding to initial temperatures of a few eV, the adiabatic cooling drives the system into a metastable region of the phase diagram, resulting in the production of a relatively large fraction of nanoparticles through phase decomposition processes.[8,12] On the other hand, at larger laser intensities ($\geqslant10^{14}$ W/cm^2) the system can never reach the metastable region of the phase diagram, resulting in an almost fully atomized plume. Thus the most promising laser intensity range in the context of nanoparticles production is predicted to be 10^{12}–10^{13} W/cm^2, and these values turn out to be in very good quantitative agreement with those leading to an efficient generation of nanoparticles for the different materials investigated in our experiments (see Table I).

In conclusion, by analyzing the fs laser produced plume for different materials we have experimentally ascertained that the process of matter removal during ultrashort (fs) laser pulse irradiation followed by vacuum expansion is characterized by a number of general features, whichever the nature of the target material. In particular, fs laser ablation of solid targets at laser intensities of the order of the plasma formation threshold for any given material inevitably leads to the generation of nanoparticles of that material. This characteristic, which is noteworthy, has turned out to be true not only

for monocomponent solids but also for multicomponent targets, is a point of extreme interest in the basic field of nanophysics, and in view of possible technological applications for nanodevices. The measured nanoparticles emission spectra during their free expansion into vacuum are fairly good described by Plank's black-body-like curves (modified for small particles) with initial temperatures of the order of few thousands K, which rapidly decreases as a function of the distance from the target surface mainly because of radiative cooling.

AFM analysis of the removed matter deposited onto mica substrates has shown that the produced nanoparticles have mean radii generally in the range 5–25 nm, with pretty narrow size distributions characterized by a standard-deviation/radius ranging from 0.5 to 0.8. The formation of these nanoparticles is likely to occur as a consequence of the complex relaxation dynamics of the extreme material state induced by intense, ultrashort laser irradiation of the target, and this specific feature evidenced by our results is in very good agreement with the physical description and numerical predictions of the recently published theoretical analyses of fs ablation processes.

[1] R. H. Baughman, A. A. Zakhidov, and W. A. de Heer, Science **297**, 787 (2002).
[2] A. S. Edelstein and R. C. Cammarata, *Nanomaterials: Synthesis, Properties and Applications* (Institute of Physics Publishing, Bristol, 1996).
[3] M. S. Gudiksen, L. J. Laudon, J. Wang, D. C. Smith, and C. M. Lieber, Nature (London) **415**, 617 (2002).
[4] C. J. Zhong and M. M. Maye, Adv. Mater. (Weinheim, Ger.) **13**, 1507 (2001).
[5] K. Sturm, S. Fahler, and H. U. Krebs, Appl. Surf. Sci. **154-155**, 492 (2003).
[6] P. P. Pronko, Z. Zhang, and P. A. VanRompay, Appl. Surf. Sci. **208-209**, 492 (2003).
[7] S. Amoruso, R. Bruzzese, N. Spinelli, R. Velotta, M. Vitiello, X. Wang, G. Ausanio, V. Iannotti, and L. Lanotte, Appl. Phys. Lett. **84**, 4502 (2004).
[8] S. Eliezer, N. Eliaz, E. Grossman, D. Fisher, I. Gouzman, Z. Henis, S. Pecker, Y. Horovitz, M. Fraenkel, S. Maman, and Y. Lereah, Phys. Rev. B **69**, 144119 (2004).
[9] O. Albert, S. Roger, Y. Glinec, J. C. Loulergue, J. Etcheparre, C. Boulmer-Leborgne, J. Perriere, and E. Millon, Appl. Phys. A: Mater. Sci. Process. **76**, 319 (2003).
[10] T. E. Glover, J. Opt. Soc. Am. B **20**, 125 (2003).
[11] K. Sokolowski-Tinten, J. Bialkowski, A. Cavalleri, D. von der Linde, A. Oparin, J. Meyer-ter-Vehn, and S. I. Anisimov, Phys. Rev. Lett. **81**, 224 (1998).
[12] F. Vidal, T. W. Johnston, S. Laville, O. Barthelemy, M. Chaker, B. Le Drogoff, J. Margot, and M. Sabsabi, Phys. Rev. Lett. **86**, 2573 (2001).
[13] D. Perez and L. J. Lewis, Phys. Rev. B **67**, 184102 (2003).
[14] P. Lorazo, L. J. Lewis, and M. Meunier, Phys. Rev. Lett. **91**, 225502 (2003).
[15] S. Amoruso, R. Bruzzese, N. Spinelli, R. Velotta, M. Vitiello, and X. Wang, Europhys. Lett. **67**, 404 (2004).